

INFINITELY MANY STANDARD TRISECTION DIAGRAMS FOR GLUCK TWISTING

TSUKASA ISOSHIMA

ABSTRACT. Gay and Meier asked if a trisection diagram for the Gluck twist on a spun or twist-spun 2-knot in S^4 obtained by a certain method is standard. In this paper, we show that the trisection diagram for the Gluck twist on the spun $(p + 1, p)$ -torus knot is standard, where p is any integer greater than or equal to 2.

1. INTRODUCTION

A trisection, which was introduced by Gay and Kirby [GK16], is roughly a decomposition of a closed oriented smooth 4-manifold into three 4-dimensional 1-handlebodies, namely, the union of a 0-handle and 1-handles. A trisection is a 4-dimensional analogue of a Heegaard splitting which is well known as a decomposition of a 3-manifold into two 3-dimensional 1-handlebodies. As well as the decomposition of a Heegaard splitting is described by a Heegaard diagram, the decomposition of a trisection is described by a trisection diagram. It is a 4-tuple which consists of a closed oriented surface appears as the triple intersection of the decomposition and three kinds of simple closed curves α , β and γ in the surface. A trisection diagram actually can be defined regardless of a trisection, but there is a one to one correspondence between trisections and trisection diagrams under an appropriate equivalence relation. A trisection diagram recovers a handle decomposition of the 4-manifold by producting a 2-dimensional disk to the surface and attaching 2-handles along the α , β and γ curves with the surface framings.

It is known as a corollary from the existence and uniqueness of trisections up to stabilization that two closed 4-manifolds are diffeomorphic if and only if two corresponding trisection diagrams are related by surface diffeomorphisms, handle slides among the same family curves and stabilizations. In the three operations, stabilizations are subtle ones since they may be not necessary in the corollary. For example, 4-manifolds obtained by spinning Seifert fibered spaces admit infinitely many trisection diagrams that they have the same genus but stabilizations are really necessary to deform one to another [Isl21]. On the other hand, it is easy to check that the two trisection diagrams of $\mathbb{C}P^2 \# \overline{\mathbb{C}P^2}$ and $S^2 \tilde{\times} S^2$, the non-trivial sphere bundle over the sphere, depicted in [GK16] are related without stabilizations. With respect to S^4 , it is conjectured, called the 4-dimensional Waldhausen conjecture, that each trisection of S^4 is isotopic to the genus 0 trisection or its stabilization [MSZ16]. This conjectures in terms of trisection diagrams (diffeomorphic level) that each trisection diagram \mathcal{D} of S^4 is related to the stabilization of the genus 0 trisection diagram (whose type is the same as the type of \mathcal{D}) without stabilizations. Actually, there are some supporting evidences of the conjecture (for example, [Iso22, MSZ16]). However, this conjecture is thought negatively at present by [MSZ16],

and there are some potential counterexamples. In this paper, as one of the potential counterexamples, we will deal with trisections of Gluck twisted 4-manifolds which are diffeomorphic to S^4 .

The Gluck twist is a cutting and pasting operation on a 2-knot. Let X be a closed 4-manifold and K be a 2-knot in X with normal Euler number 0. Then, the Gluck twisted 4-manifold $\Sigma_K(X) = X - \text{int}(\nu(K)) \cup_{\tau} S^2 \times D^2$, where τ is the non-trivial self-diffeomorphism of $S^2 \times S^1$, namely $\tau(z, e^{i\theta}) = (ze^{i\theta}, e^{i\theta})$, and $\nu(K)$ is a tubular neighborhood of K in X . If $X = S^4$, the Gluck twisted 4-manifold on any 2-knot is a homotopy 4-sphere, and hence homeomorphic to S^4 by Freedman's theorem. Moreover, it is well-known that the 4-manifold is diffeomorphic to S^4 if K is a spun 2-knot or twist-spun 2-knot. Thus, a corresponding trisection diagram and the stabilization of the genus 0 trisection diagram are related by the 3-operations including stabilizations. However, it is not known that whether stabilizations are truly necessary for its deformation or not. Gay and Meier submitted a question about it as follows: Note we say that a trisection diagram of a 4-manifold which is diffeomorphic to S^4 is *standard* if it is the stabilization of the genus 0 trisection diagram after several surface diffeomorphisms and handle slides.

Question 1.1 ([GM22]). Let \mathcal{K} be the spin or the twist-spin of a non-trivial knot K in S^3 . Is a trisection diagram of $\Sigma_{\mathcal{K}}(S^4)$ constructed from a doubly-pointed Heegaard diagram of K by combining some methods **ever** standard?

The trisection diagram in the question might be considered non-standard. If it is true, the trisection diagram is a counterexample of the conjecture mentioned above. However, as one of the main theorems in [IO23], the author and Ogawa showed that if we choose the trefoil as the 1-knot K and Figure 2 except δ_1 and δ_2 as its doubly-pointed Heegaard diagram, then the trisection diagram is standard. In this paper, we show the following main theorem including this theorem.

Theorem (Theorem 4.1). *The trisection diagram \mathcal{D}_p ($p \geq 2$) is standard.*

The trisection diagram \mathcal{D}_p is the one depicted in Figure 8. This is the trisection diagram in Question 1.1 when we choose $(p+1, p)$ -torus knot and Figure 2 as K and its doubly-pointed Heegaard diagram, respectively. In the proof of the theorem, we perform so many Dehn twists and handle slides. In the final step of the proof, we use an inductive argument for trisection diagrams, which we call the seesaw lemma (Lemma 4.7).

ORGANIZATION

We briefly review preliminaries, specifically (relative) trisections of 4-manifolds (with boundary) and doubly pointed Heegaard/trisection diagrams in Section 2. In Section 3, we construct the trisection diagram in the question for the spun $(p+1, p)$ -torus knot explicitly by the methods mentioned in the question. Then we prove the main theorem in Section 4. We have further remarks in Section 5.

ACKNOWLEDGEMENT

The author would like to express sincere gratitude to his supervisor, Hisaaki Endo, for his helpful comments. The author is partially supported by Grant-in-Aid for JSPS Research Fellow from JSPS KAKENHI Grant Number JP23KJ0888.

2. PRELIMINARIES

In this section, we review notions used in Section 3 and 4. In this paper, unless otherwise stated, any 4-manifold is compact, connected, oriented and any surface-knot is a connected, closed surface smoothly embedded in a 4-manifold. A more detailed description of the notions appeared in this section is given in Section 2 in [IO23].

2.1. Trisections and relative trisections. In this subsection, we recall (relative) trisections of 4-manifolds (with boundary).

Definition 2.1. Let X be a closed 4-manifold. A $(g; k_1, k_2, k_3)$ -trisection of X is a 3-tuple (X_1, X_2, X_3) satisfying the following conditions:

- $X = X_1 \cup X_2 \cup X_3$,
- For each $i = 1, 2, 3$, $X_i \cong \natural_{k_i} S^1 \times D^3$,
- For each $i = 1, 2, 3$, $X_i \cap X_j \cong \natural_g S^1 \times D^2$,
- $X_1 \cap X_2 \cap X_3 \cong \#_g S^1 \times S^1 = \Sigma_g$.

Let $H_\alpha = X_3 \cap X_1$, $H_\beta = X_1 \cap X_2$ and $H_\gamma = X_2 \cap X_3$. The union $H_\alpha \cup H_\beta \cup H_\gamma$ is called the *spine* of the trisection. A trisection is uniquely determined by its spine. Note that if $k_1 = k_2 = k_3$, the trisection is said to be *balanced*. In Section 1, the 4-tuple of non-negative integers $(g; k_1, k_2, k_3)$ is called the *type* of the trisection.

The decomposition of a trisection is described by a trisection diagram.

Definition 2.2. A 4-tuple $(\Sigma_g, \alpha, \beta, \gamma)$ is called a $(g; k_1, k_2, k_3)$ -trisection diagram if the following holds:

- $(\Sigma_g, \alpha, \beta)$ is a Heegaard diagram of $\#_{k_1} S^1 \times S^2$,
- $(\Sigma_g, \beta, \gamma)$ is a Heegaard diagram of $\#_{k_2} S^1 \times S^2$,
- $(\Sigma_g, \gamma, \alpha)$ is a Heegaard diagram of $\#_{k_3} S^1 \times S^2$.

Definition 2.3. A *stabilization* of a trisection diagram is the connected-sum of the trisection diagram and the genus 1 trisection diagram of S^4 depicted in Figure 1, or the trisection diagram itself obtained by the connected-sum. The reverse operation is called a *destabilization*.

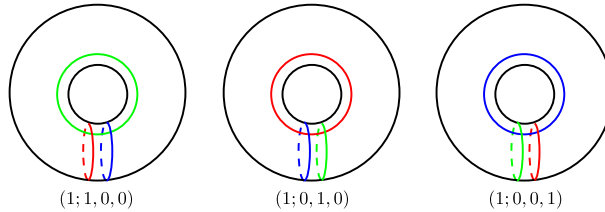


Figure 1. The genus 1 trisection diagrams of S^4 .

Note that this (de)stabilization is the unbalanced one.

Any 4-manifold admits a trisection, and any two trisections of the same 4-manifold is isotopic after stabilizing them balancedly some times [GK16]. As a corollary, it is known that any two closed 4-manifolds are diffeomorphic if and only if corresponding two trisection diagrams are related by surface diffeomorphisms, handle slides among the same family curves and balanced stabilizations.

Let X and Y be diffeomorphic closed 4-manifolds. Two trisections (X_1, X_2, X_3) of X and (Y_1, Y_2, Y_3) of Y are *diffeomorphic* if there exists a diffeomorphism $h: X \rightarrow Y$ such that $h(X_i) = Y_i$ for each $i = 1, 2, 3$. Two trisections (X_1, X_2, X_3) and (Y_1, Y_2, Y_3) of a 4-manifold Z are *isotopic* if there exists an isotopy $h_t: Z \rightarrow Z$ such that $h_0 = id_Z$ and $h_1(X_i) = Y_i$ for each $i = 1, 2, 3$. Two trisections are diffeomorphic if and only if corresponding two trisection diagrams are related without stabilizations. It is conjectured that any trisection of S^4 is isotopic to the genus 0 trisection or its stabilization [MSZ16]. A counterexample of this conjecture may be given via trisection diagrams of a 4-manifold diffeomorphic to S^4 since any two isotopic trisections are diffeomorphic.

Trisections of 4-manifolds with boundary are called *relative trisections* [Cas16]. As well as the closed case, *relative trisection diagrams* can be defined for relative trisections [CGPC18]. *Arced relative trisection diagrams*, which are needed when we consider gluing two relative trisection diagrams, are defined for relative trisection diagrams. An algorithm for drawing the arcs is developed (Theorem 5 in [CGPC18]).

2.2. Doubly pointed Heegaard/trisection diagrams. A *b-bridge decomposition* is a decomposition of a classical knot in a 3-manifold using its Heegaard splitting such that the knot intersects each handlebody in b trivial arcs. A knot admits a 1-bridge decomposition can be described by a *doubly pointed Heegaard diagram* which is a Heegaard diagram of the 3-manifold with two base points. The union of two arcs connecting the two base points in each handlebody of the Heegaard splitting describes the knot, and a knot can be determined uniquely by the two base points. For more details, see [Ord13] for example.

As well as bridge decompositions of classical knots in 3-manifolds, *bridge trisections* of surface knots in 4-manifolds are introduced in [MZ17, MZ18]. A bridge trisected surface-knot in any 4-manifold can be described by its *shadow diagram* that is a pair of a trisection diagram of the 4-manifold and arcs describing the surface-knot. In particular, a shadow diagram of a 2-knot which is 1-bridge position is called a *doubly pointed trisection diagram*. This is a pair of a trisection diagram and two points describing the 2-knot, often denoted $(\Sigma, \alpha, \beta, \gamma, z, w)$. Note it is known that each 2-knot can be put in 1-bridge position by meridional stabilizations [MZ17, MZ18]. See [MZ17, MZ18] for more details.

3. CONSTRUCTING TRISECTION DIAGRAMS FOR GLUCK TWISTING

In this section, we construct the trisection diagram (Lemma 3.3) in Question 1.1 for the spun $(p+1, p)$ -torus knot $S(t(p+1, p))$. Since the way of the construction is the same as it in Section 3 in [IO23], we omit some explanations that should be done.

Lemma 3.1. *Let $(\Sigma, \alpha, \beta, z, w)$ be a doubly-pointed Heegaard diagram of $(S^3, t(3, 2))$ depicted in Figure 2. Then, for $p \geq 2$, $(\Sigma, \alpha, t_{\delta_1}^{p-2} t_{\delta_2}^{-(p-2)}(\beta), z, w)$ is a doubly-pointed Heegaard diagram of $(S^3, t(p+1, p))$, where δ_1 and δ_2 are the curves depicted in Figure 2.*

Proof. It is easily seen that $(\Sigma, \alpha, t_{\delta_1} t_{\delta_2}^{-1}(\beta), z, w)$ is a doubly-pointed Heegaard diagram of $(S^3, t(4, 3))$, and hence we inductively see that $(\Sigma, \alpha, t_{\delta_1}^{p-2} t_{\delta_2}^{-(p-2)}(\beta), z, w)$ is a doubly-pointed Heegaard diagram of $(S^3, t(p+1, p))$. See also [Ord13]. \square

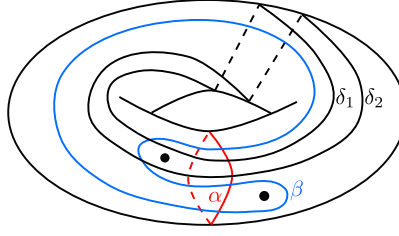


Figure 2. A doubly-pointed Heegaard diagram of $(S^3, t(3, 2))$ and the curves δ_1 and δ_2 .

We have the following arced relative trisection diagram of $S^4 - S(t(p+1, p))$ from this doubly-pointed Heegaard diagram by Meier's spinning method, removing the base points of the doubly-pointed trisection diagram and an algorithm for drawing arcs of the relative trisection diagram. See Section 3 in [IO23] for details.

Lemma 3.2. *Let $(\Sigma, \alpha, \beta, \gamma, a, b, c)$ be an arced relative trisection diagram of $S^4 - S(t(3, 2))$ depicted in Figure 3. Then, for $p \geq 2$, $(\Sigma, \alpha', \beta', \gamma', a', b', c')$ is an arced relative trisection diagram of $S^4 - S(t(p+1, p))$, where*

- $\alpha' = (t_{\delta_1^\beta}^{p-2} t_{\delta_2^\beta}^{-(p-2)})(\alpha_1, \alpha_2, \alpha_3)$,
- $\beta' = (t_{\delta_1^\beta}^{p-2} t_{\delta_2^\beta}^{-(p-2)})(\beta_1, \beta_2, \beta_3)$,
- $\gamma' = (t_{\delta_1^\gamma}^{p-2} t_{\delta_2^\gamma}^{-(p-2)})(\gamma_1, \gamma_2, \gamma_3)$,
- $a' = t_{\delta_1^\beta}^{p-2} t_{\delta_2^\beta}^{-(p-2)}(a)$,
- $b' = t_{\delta_1^\beta}^{p-2} t_{\delta_2^\beta}^{-(p-2)}(b)$,
- $c' = t_{\delta_1^\gamma}^{p-2} t_{\delta_2^\gamma}^{-(p-2)}(c)$,

and the curves δ_1^β , δ_2^β , δ_1^γ and δ_2^γ are them depicted in Figure 3.

Gay and Meier [GM22] showed that a trisection diagram of $\Sigma_K(X)$ is obtained by gluing an arced relative trisection diagram of the exterior of K and Figure 4a. Thus, we can have the required trisection diagram as in the following lemma.

Lemma 3.3. *Let $(\Sigma, \alpha, \beta, \gamma)$ be a trisection diagram obtained by Gluck twisting on the spun trefoil depicted in Figure 5, using the methods of [GM22]. Then, for $p \geq 2$, $(\Sigma, \alpha', \beta', \gamma')$ is a trisection diagram obtained by Gluck twisting on $S(t(p+1, p))$ using the same methods, where*

- $\alpha' = (t_{\delta_1^\beta}^{p-2} t_{\delta_2^\beta}^{-(p-2)})(\alpha_1, \alpha_2, \alpha_3, t_{\delta_1^\beta}^{p-2} t_{\delta_2^\beta}^{-(p-2)})(\alpha_4, \alpha_5, \alpha_6)$,
- $\beta' = (t_{\delta_1^\beta}^{p-2} t_{\delta_2^\beta}^{-(p-2)})(\beta_1, \beta_2, \beta_3, t_{\delta_1^\beta}^{p-2} t_{\delta_2^\beta}^{-(p-2)})(\beta_4, \beta_5, \beta_6)$,
- $\gamma' = (t_{\delta_1^\gamma}^{p-2} t_{\delta_2^\gamma}^{-(p-2)})(\gamma_1, \gamma_2, \gamma_3, t_{\delta_1^\gamma}^{p-2} t_{\delta_2^\gamma}^{-(p-2)})(\gamma_4, \gamma_5, \gamma_6)$,

and the curves δ_1^β , δ_2^β , δ_1^γ and δ_2^γ are them depicted in Figure 5.

In this paper, we show in Section 4 that this trisection diagram is standard for all $p \geq 2$. So, we may destabilize this trisection diagram at this time if we can do it. Destabilizing Figure 4a twice can provide us with one of Figure 4b. Thus, it suffices to show that Figure 6 is standard, which is obtained by gluing Figure 3 and

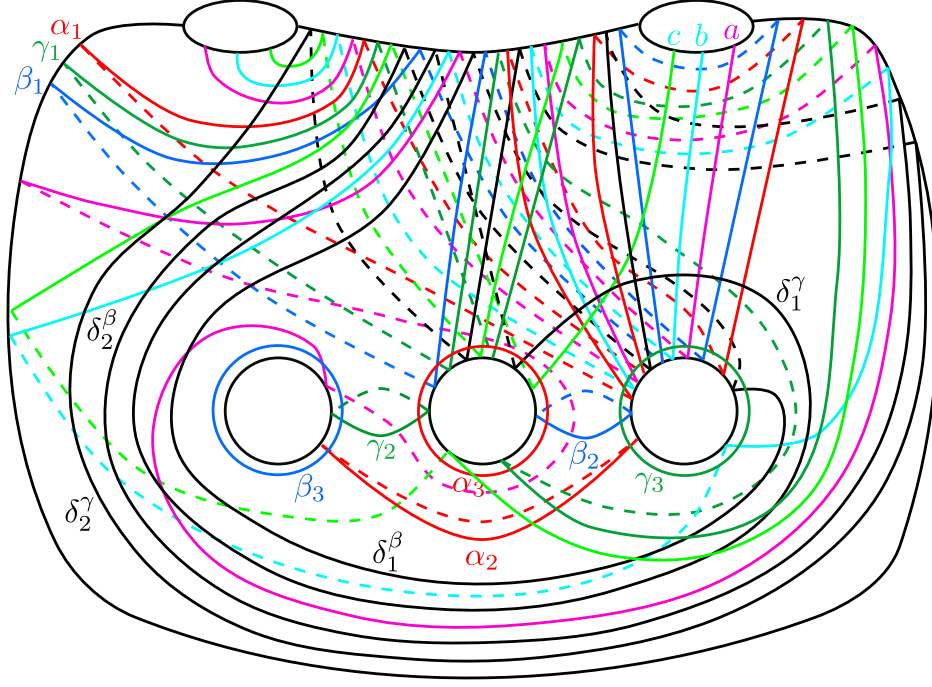


Figure 3. An arced relative trisection diagram of $S^4 - S(t(3, 2))$ and the curves δ_1^β , δ_2^β , δ_1^γ and δ_2^γ .

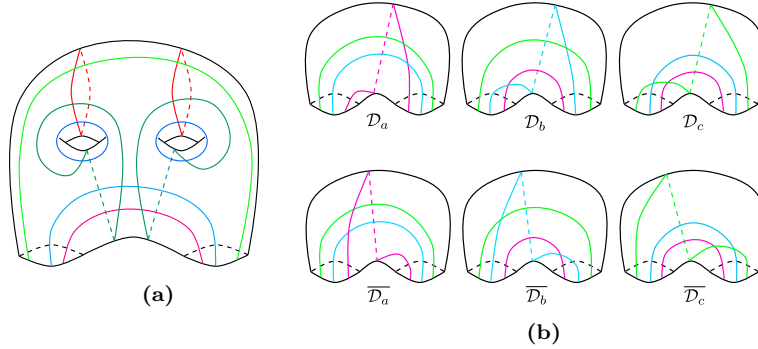


Figure 4. The diagrams used in the construction of a trisection diagram of a Gluck twisted 4-manifold.

$\overline{D_b}$ in Figure 4b. Note that we depict Figure 7 as the α , β and γ curves in Figure 6 for clarity.

Let $c_1 \rightarrow c_2$ denote a handle slide c_1 over c_2 . In Figure 6 or 7, we perform the following handle slides, namely, $\alpha_4 \rightarrow \alpha_3$, $\alpha_1 \rightarrow (\alpha_2, \alpha_3)$, $\alpha_4 \rightarrow \alpha_1$, $\alpha_4 \rightarrow \alpha_3$ twice, $\beta_4 \rightarrow \beta_1$, $\beta_1 \rightarrow \beta_4$, and $\gamma_4 \rightarrow \gamma_1$ twice. Then, Figure 8 is obtained.

Let \mathcal{D}_p denote this trisection diagram of $\Sigma_{S(t(p+1,p))}(S^4)$, which is obtained by overlaying all of Figure 8.

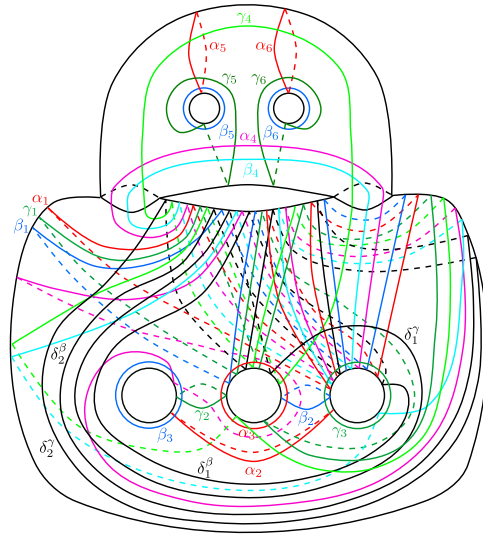


Figure 5. A trisection diagram obtained by Gluck twisting on the spun trefoil and the curves $\delta_1^\beta, \delta_2^\beta, \delta_1^\gamma$ and δ_2^γ .

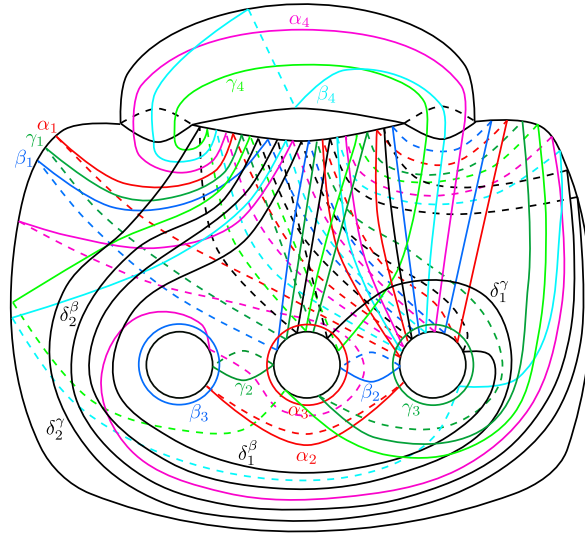


Figure 6. A trisection diagram obtained by Gluck twisting on the spun trefoil and the curves $\delta_1^\beta, \delta_2^\beta, \delta_1^\gamma$ and δ_2^γ .

4. MAIN THEOREM

In this section, we show the following main theorem which is mentioned in Section 1.

Theorem 4.1. *The trisection diagram \mathcal{D}_p ($p \geq 2$) is standard.*

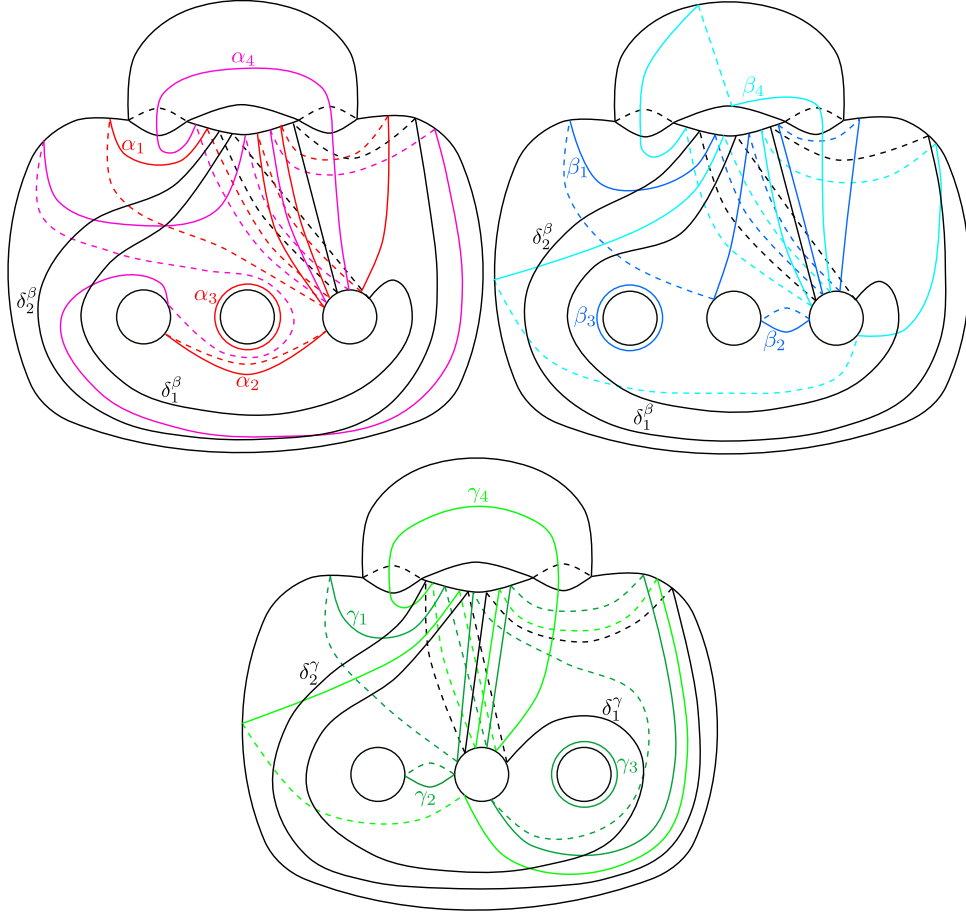


Figure 7. These diagrams depict the α , β and γ curves in Figure 6 for visual clarity.

Remark 4.2. The key idea of the proof is handle sliding curves used when we perform Dehn twists over each family curves. See Figure 9 for details.

We prove this theorem by deforming \mathcal{D}_p step by step. The proof is mainly divided into three steps: The first step is deforming the trisection diagram appropriately so that we can destabilize it. The second step is destabilizing the trisection diagram in the first step. The last step is that we reduce the destabilized trisection diagram to the stabilization of the genus 0 trisection diagram by an inductive argument. As the inductive argument, we use a key lemma which we call the seesaw lemma. Note that we do not change names of simple closed curves before and after Dehn twists and handle slidings.

step1: Deform \mathcal{D}_p so that we can destabilize it. First, we deform the β -curves to destabilize the trisection diagram.

Lemma 4.3. *Let $(\Sigma; \beta_1^p, \beta_2^p, \beta_3^p, \beta_4^p)$ be the β -curves in \mathcal{D}_p . Then, the following holds for β_1^p and β_4^p :*

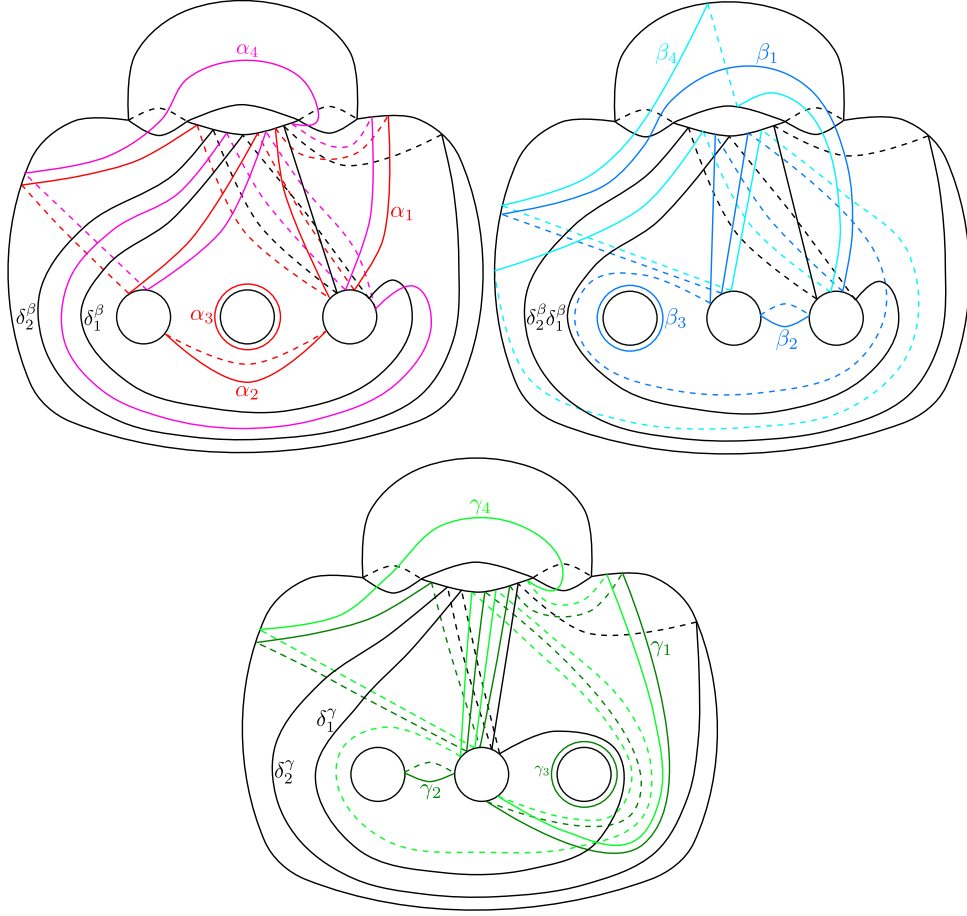


Figure 8. The trisection diagram \mathcal{D}_p of $\Sigma_{S(t(p+1,p))}(S^4)$.

- $t_\epsilon^{p-2} t_\delta^{-1}(\beta_4^p) = m$,
- $t_\epsilon^{p-2} t_\delta^{-1}(\beta_1^p) = t_{\delta_1^{\beta}}^{p-2}(m')$ up to handle slide over β_2 and β_3 ,

where $\beta_2, \beta_3, \delta_1^\beta, \delta, \epsilon, m$ and m' are the curves depicted in Figure 10.

Proof. First of all, we show the former statement. Since $m = t_\delta^{-1}(\beta_4)$, we show $t_\epsilon^{p-2} t_\delta^{-1} t_{\delta_1^{\beta}}^{p-2} t_{\delta_2^{\beta}}^{-(p-2)}(\beta_4) = t_\delta^{-1}(\beta_4)$. Since the geometric intersection number of δ_1^β and the other curves is 0, $t_\epsilon^{p-2} t_\delta^{-1} t_{\delta_1^{\beta}}^{p-2} t_{\delta_2^{\beta}}^{-(p-2)}(\beta_4) = t_{\delta_1^{\beta}}^{p-2} t_\epsilon^{p-2} t_\delta^{-1} t_{\delta_2^{\beta}}^{-(p-2)}(\beta_4)$. Then,

$$\begin{aligned}
 t_{\delta_1^{\beta}}^{p-2} t_\epsilon^{p-2} t_\delta^{-1} t_{\delta_2^{\beta}}^{-(p-2)}(\beta_4) &= t_{\delta_1^{\beta}}^{p-2} t_\delta^{-1} t_\delta t_\epsilon^{p-2} t_\delta^{-1} t_{\delta_2^{\beta}}^{-(p-2)}(\beta_4) \\
 &= t_{\delta_1^{\beta}}^{p-2} t_\delta^{-1} t_{t_\delta(\epsilon)}^{p-2} t_{\delta_2^{\beta}}^{-(p-2)}(\beta_4) \\
 &= t_{\delta_1^{\beta}}^{p-2} t_\delta^{-1} t_{\delta_2^{\beta}}^{p-2} t_{\delta_2^{\beta}}^{-(p-2)}(\beta_4) \\
 &= t_\delta^{-1} t_{\delta_1^{\beta}}^{p-2}(\beta_4).
 \end{aligned}$$

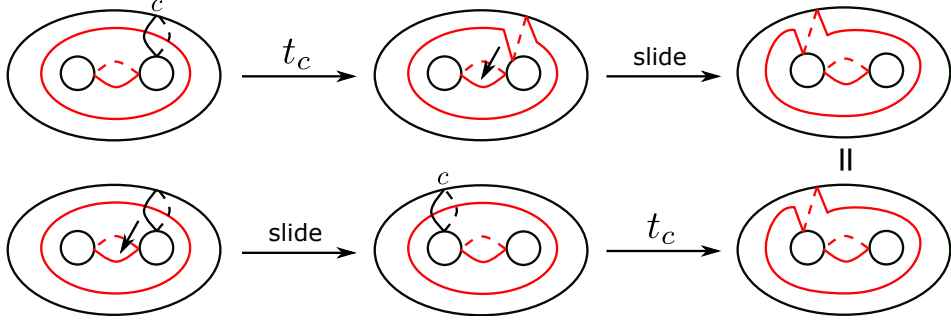


Figure 9. This figure describes a simple example of the key idea of the proof of Theorem 4.1. In the upper column, we perform firstly the Dehn twist, and then handle sliding. This is a usual deformation for tisection diagrams. In the lower column which describes a new deformation, we firstly handle slide c over the α curve, and then perform the Dehn twist. The resulting two diagrams are the same.

Thus, it suffices to show $t_\delta^{-1}t_{\delta_1}^{p-2}(\beta_4) = t_\delta^{-1}(\beta_4)$. This holds obviously since $i(\delta_1^\beta, \beta_4) = 0$, where $i(\delta_1^\beta, \beta_4)$ is the geometric intersection number of δ_1^β and β_4 .

Next, we show the latter statement.

$$\begin{aligned}
t_{\delta_1}^{-(p-2)}t_\epsilon^{p-2}t_\delta^{-1}(\beta_1^p) &= t_{\delta_1}^{-(p-2)}t_\epsilon^{p-2}t_\delta^{-1}t_{\delta_1}^{p-2}t_{\delta_2}^{-(p-2)}(\beta_1) \\
&= t_\delta^{-1}t_\delta t_\epsilon^{p-2}t_\delta^{-1}t_{\delta_2}^{-(p-2)}(\beta_1) \\
&= t_\delta^{-1}t_{t_\delta(\epsilon)}^{p-2}t_{\delta_2}^{-(p-2)}(\beta_1) \\
&= t_\delta^{-1}t_{\delta_2}^{p-2}t_{\delta_2}^{-(p-2)}(\beta_1) \\
&= t_\delta^{-1}(\beta_1).
\end{aligned}$$

We see from Figure 10 that $t_\delta^{-1}(\beta_1)$ can be parallel to m' after handle sliding over both β_2 and β_3 . \square

In Lemma 4.3, since we perform $t_\epsilon^{p-2}t_\delta^{-1}$ for the β curves in Figure 8, we must perform the Dehn twists for the α and γ curves in Figure 8. Before deforming the α curves, we define the following operation including the Dehn twists, which we call $*$: First, perform t_δ^{-1} . Then, slide α_1 over α_3 only once to resolve the intersection of α_1 and ϵ (see the left figure in Figure 11). After that, perform t_ϵ^{p-2} . Finally, slide α_1 and α_3 over α_4 $p-1$ times each to resolve the intersections of m and both α_1 and α_3 (see the right figure in Figure 11).

Lemma 4.4. *The α curves $(t_{\delta_1}^{p-2}t_{\tilde{\delta}}^{-(p-2)}(\alpha_1), \alpha_2, t_{\delta_1}^{p-2}t_{\tilde{\delta}}^{p-2}(\alpha_3), t_{\delta_1}^{p-2}(\alpha_4))$ can be obtained by performing the operation $*$ for the α curves in Figure 8, where $\alpha_1, \alpha_3, \hat{\delta}$ and $\tilde{\delta}$ are the curves depicted in Figure 12.*

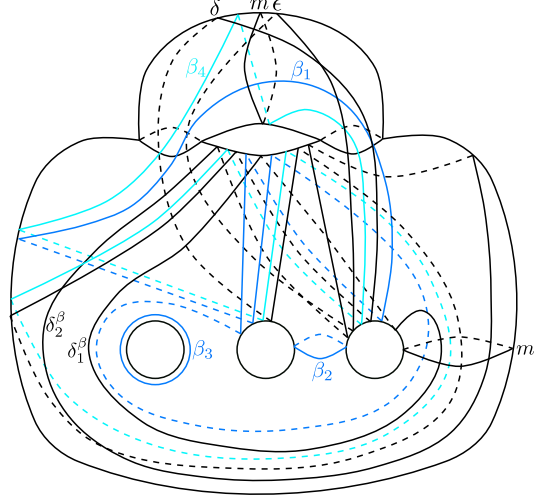


Figure 10. The β curves obtained by $t_\epsilon^{p-2}t_\delta^{-1}$ for the β curves in Figure 8.

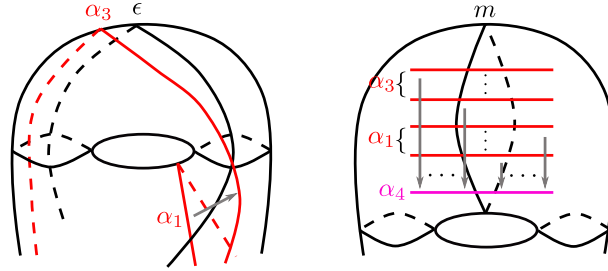


Figure 11. These figures describe how to perform the handle slides in the operation $*$.

Proof. It is obvious that $t_{\delta_1^\beta}^{p-2}(\alpha_4)$ is obtained by $*$ since both δ and ϵ do not intersect α_4 . We show firstly the statement for α_1 . The operations which deform α_1 in Figure 8 are as follows:

$$t_{\delta_2^\beta}^{-(p-2)} \rightarrow t_\delta^{-1} \rightarrow (\rightarrow t_\delta^{-1}(\alpha_3) \text{ in Figure 8}) \rightarrow (\rightarrow \alpha_4 \text{ } p-1 \text{ times}) \rightarrow t_{\delta_1^\beta}^{p-2}.$$

Note that this means α_1 in Figure 8 is deformed in order by $t_{\delta_2^\beta}^{-(p-2)}$, t_δ^{-1} , handle sliding over $t_\delta^{-1}(\alpha_3)$ in Figure 8, handle sliding over α_4 and $t_{\delta_1^\beta}^{p-2}$. Since $t_\delta^{-1}t_{\delta_2^\beta}^{-(p-2)} = t_{t_\delta^{-1}(\delta_2^\beta)}^{-(p-2)}t_\delta^{-1}$, we can take the following operations instead of the above operations:

$$t_\delta^{-1} \rightarrow t_{t_\delta^{-1}(\delta_2^\beta)}^{-(p-2)} \rightarrow (\rightarrow t_\delta^{-1}(\alpha_3) \text{ in Figure 8}) \rightarrow (\rightarrow \alpha_4 \text{ } p-1 \text{ times}) \rightarrow t_{\delta_1^\beta}^{p-2}.$$

Then, the first operation t_δ^{-1} does not deform α_1 in Figure 8, thus we can take the following operations:

$$t_{t_\delta^{-1}(\delta_2^\beta)}^{-(p-2)} \rightarrow (\rightarrow t_\delta^{-1}(\alpha_3) \text{ in Figure 8}) \rightarrow (\rightarrow \alpha_4 \text{ } p-1 \text{ times}) \rightarrow t_{\delta_1^\beta}^{p-2}.$$

In this operations, since $t_\delta^{-1}(\delta_2^\beta)$ does not intersect $t_\delta^{-1}(\alpha_3)$ in Figure 8, we can change the order in the operations as follows:

$$(\rightarrow t_\delta^{-1}(\alpha_3) \text{ in Figure 8}) \rightarrow t_{t_\delta^{-1}(\delta_2^\beta)}^{-(p-2)} \rightarrow (\rightarrow \alpha_4 \text{ } p-1 \text{ times}) \rightarrow t_{\delta_1^\beta}^{p-2}.$$

Handle sliding α_1 over $t_\delta^{-1}(\alpha_3)$ and α_4 in Figure 8 provides us with α_1 in Figure 12a up to handle slide over α_2 . Thus, the remaining operations for α_1 in Figure 12a are as follows:

$$t_{t_\delta^{-1}(\delta_2^\beta)}^{-(p-2)} \rightarrow (\rightarrow \alpha_4 \text{ } p-2 \text{ times}) \rightarrow t_{\delta_1^\beta}^{p-2}.$$

Since $t_\delta^{-1}(\delta_2^\beta)$ does not intersect α_4 , the operations $t_{t_\delta^{-1}(\delta_2^\beta)}^{-(p-2)} \rightarrow (\rightarrow \alpha_4 \text{ } p-2 \text{ times})$ can be regarded as $t_c^{-(p-2)}$, where c is the simple closed curve obtained by $t_\delta^{-1}(\delta_2^\beta) \rightarrow \alpha_4$. Actually, c is $\hat{\delta}$. This completes the proof for α_1 .

Next, we show the statement for α_3 . In the second operation and $*$ in the proof for α_1 , the operations which deform α_3 in Figure 8 are as follows:

$$t_\delta^{-1} \rightarrow t_{\epsilon}^{p-2} \rightarrow (\rightarrow \alpha_4 \text{ } p-1 \text{ times}) \rightarrow t_{\delta_1^\beta}^{p-2}.$$

We can regard this operations as the following operations, namely

$$t_{c_1}^{-1} \rightarrow t_{c_2}^{p-2} \rightarrow t_{\delta_1^\beta}^{p-2},$$

where c_1 is the simple closed curve obtained by handle sliding δ over α_4 and c_2 is the simple closed curve obtained by handle sliding ϵ over α_4 . It is obvious that $t_{c_1}^{-1}(\alpha_3)$ in Figure 8 is α_3 in Figure 12b and c_2 is $\tilde{\delta}$. This completes the proof for α_3 . \square

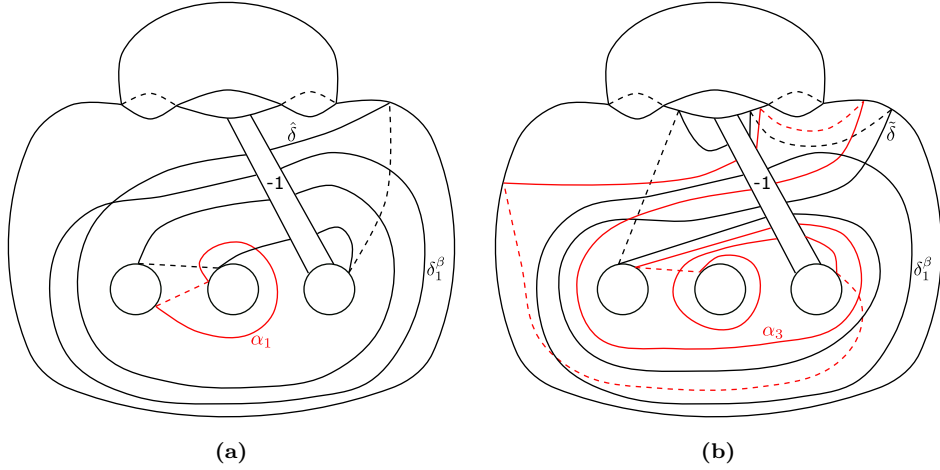


Figure 12. A part of the α curves obtained by the operation $*$ for the α curves in Figure 8. See Figure 13 on the (-1) -box notation.

Next, we perform $t_\epsilon^{p-2}t_\delta^{-1}$ for the γ curves in Figure 8. Before deforming the γ curves, we define the following operation including the Dehn twists, which we call $**$: First, perform t_δ^{-1} and t_ϵ^{p-2} . Then, slide $t_\epsilon^{p-2}t_\delta^{-1}(\gamma_3)$ in Figure 8 over $t_{\delta_1^\beta}^{p-2}(\gamma_4)$

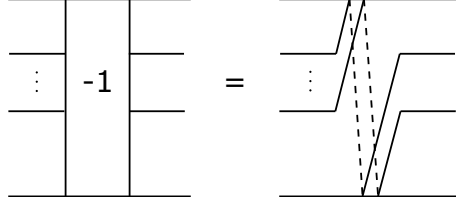


Figure 13. A new simple notation for trisection diagrams based on the twist-box notations in Kirby diagrams. This notation simplifies the left-handed Dehn twist.

only once to resolve the intersection with m . The way of performing the handle slide is the same as the last slide in the operation $*$ (see the right figure in Figure 11).

Lemma 4.5. *The γ curves $(t_{\delta_1^\gamma}^{p-2}(\gamma_1), \gamma_2, t_{\delta_1^\gamma}^{p-2}(\gamma_3), t_{\delta_1^\gamma}^{p-2}(\gamma_4))$ can be obtained by performing the operation $**$ for the γ curves in Figure 8, where γ_1, γ_3 , and δ_1^γ are the curves depicted in Figure 14.*

Proof. Since

$$\begin{aligned} t_\epsilon^{p-2} t_\delta^{-1} t_{\delta_1^\gamma}^{p-2} t_{\delta_2^\gamma}^{-(p-2)} &= t_{\delta_1^\gamma}^{p-2} t_\epsilon^{p-2} t_\delta^{-1} t_{\delta_2^\gamma}^{-(p-2)} \\ &= t_{\delta_1^\gamma}^{p-2} t_\delta^{-1} t_{t_\delta(\epsilon)}^{p-2} t_{\delta_2^\gamma}^{-(p-2)} \\ &= t_{\delta_1^\gamma}^{p-2} t_\delta^{-1} t_{\delta_2^\gamma}^{p-2} t_{\delta_2^\gamma}^{-(p-2)} \\ &= t_{\delta_1^\gamma}^{p-2} t_\delta^{-1}, \end{aligned}$$

the statements for $\gamma_1, \gamma_2, \gamma_4$ obviously holds. For γ_3 , we may consider the following operations:

$$t_\delta^{-1} \rightarrow t_{\delta_1^\gamma}^{p-2} \rightarrow (\rightarrow t_{\delta_1^\gamma}^{p-2}(\gamma_4) \text{ in Figure 8}).$$

We can take the following operation instead of the above operations:

$$t_\delta^{-1} \rightarrow (\rightarrow \gamma_4 \text{ in Figure 8}) \rightarrow t_{\delta_1^\gamma}^{p-2}.$$

We see that the simple closed curve obtained by handle sliding $t_\delta^{-1}(\gamma_3)$ in Figure 8 over γ_4 is γ_3 in Figure 14. This completes the proof. \square

step2: Destabilize the trisection diagram in the step1.

So, we have now the trisection diagram (α, β, γ) , where $\alpha = (t_{\delta_1^\beta}^{p-2} t_\delta^{-(p-2)}(\alpha_1), \alpha_2, t_{\delta_1^\beta}^{p-2} t_\delta^{p-2}(\alpha_3), t_{\delta_1^\beta}^{p-2}(\alpha_4))$, $\beta = (t_{\delta_1^\beta}^{p-2}(\beta_1), \beta_2, \beta_3, \beta_4 = m)$ and $\gamma = (t_{\delta_1^\gamma}^{p-2}(\gamma_1), \gamma_2, t_{\delta_1^\gamma}^{p-2}(\gamma_3), t_{\delta_1^\gamma}^{p-2}(\gamma_4))$ (see Figure 12, 10 and 14, respectively). Then, β_4 intersects both α_4 and γ_4 only once. By handle sliding α_4 and γ_4 over α_2 and γ_2 respectively, α_4 and γ_4 can be parallel. Moreover, δ_1^β and δ_1^γ can be parallel by the same handle slide. Thus, $t_{\delta_1^\beta}^{p-2}(\alpha_4)$ and $t_{\delta_1^\gamma}^{p-2}(\gamma_4)$ can be parallel (slide other curves if necessary), and we can destabilize the trisection diagram for $t_{\delta_1^\beta}^{p-2}(\alpha_4)$, β_4 and $t_{\delta_1^\gamma}^{p-2}(\gamma_4)$. Note that this destabilization is based on Naylor's method (Lemma 8 in [Nay22]). By this destabilization, we now have the trisection diagram

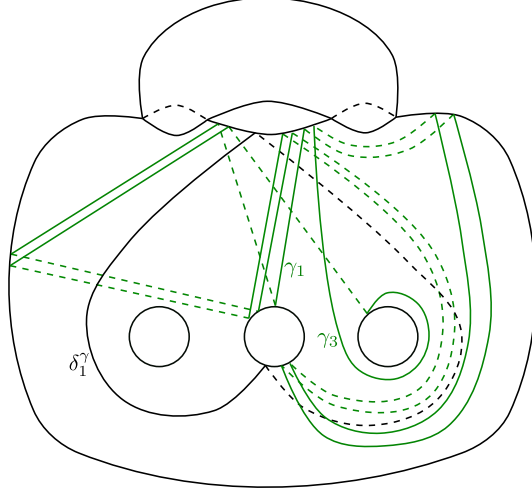


Figure 14. A part of the γ curves obtained by the operation $**$ for the γ curves in Figure 8.

(α, β, γ) depicted in Figure 15, where $\alpha = (t_{\delta_1^\beta}^{p-2} t_{\hat{\delta}}^{-(p-2)}(\alpha_1), \alpha_2, t_{\delta_1^\beta}^{p-2} t_{\hat{\delta}}^{p-2}(\alpha_3))$, $\beta = (t_{\delta_1^\beta}^{p-2}(\beta_1), \beta_2, \beta_3)$ and $\gamma = (t_{\delta_1^\gamma}^{p-2}(\gamma_1), \gamma_2, t_{\delta_1^\gamma}^{p-2}(\gamma_3))$.

step3: Reduce the destabilized trisection diagram to the stabilization of the genus 0 trisection diagram. We make some preparations to adapt the seesaw lemma (Lemma 4.7). In Figure 15, slide γ_3 over γ_1 , perform t_{β_2} for the diagram and slide α_1 over α_2 . Then, the trisection diagram (α, β, γ) depicted in Figure 16, where $\alpha = (t_{\delta_1^\beta}^{p-2} t_{\hat{\delta}}^{-(p-2)}(\alpha_1), \alpha_2, t_{\delta_1^\beta}^{p-2} t_{\hat{\delta}}^{p-2}(\alpha_3))$, $\beta = (t_{\delta_1^\beta}^{p-2}(\beta_1), \beta_2, \beta_3)$ and $\gamma = (t_{\delta_1^\gamma}^{p-2}(\gamma_1), \gamma_2, t_{\delta_1^\gamma}^{p-2}(\gamma_3))$, can be obtained. Note that we here slide δ_1^β and δ_1^γ over β_2 and the new γ_3 , respectively.

Lemma 4.6. *The trisection diagram (α, β, γ) depicted in Figure 17, where $\alpha = (\alpha_1, \alpha_2, \alpha_3)$, $\beta = (\beta_1, \beta_2, \beta_3)$ and $\gamma = t_{\hat{\delta}}^{-(p-2)} t_{\delta_1^\beta}^{p-2} t_{\delta_1^\beta}^{-(p-2)} t_{\delta_1^\gamma}^{p-2}(\gamma_1, \gamma_2, \gamma_3)$, is obtained from the above trisection diagram. Note that for a surface diffeomorphism g and a collection of simple closed curves $\gamma = (\gamma_1, \gamma_2, \gamma_3)$, $g(\gamma)$ denotes $(g(\gamma_1), g(\gamma_2), g(\gamma_3))$.*

Proof. By performing $t_{\hat{\delta}}^{-(p-2)} t_{\delta_1^\beta}^{p-2} t_{\delta_1^\beta}^{-(p-2)}$ for the above trisection diagram depicted in Figure 16, we have the trisection diagram

$$((\alpha_1, \alpha_2, \alpha_3), t_{\hat{\delta}}^{-(p-2)} t_{\delta_1^\beta}^{p-2} t_{\delta_1^\beta}^{-(p-2)} t_{\delta_1^\gamma}^{p-2}(\beta_1, \beta_2, \beta_3), t_{\hat{\delta}}^{-(p-2)} t_{\delta_1^\beta}^{p-2} t_{\delta_1^\beta}^{-(p-2)} t_{\delta_1^\gamma}^{p-2}(\gamma_1, \gamma_2, \gamma_3)).$$

By sliding α_3 over α_1 , we have the α curves in Figure 17. By sliding $\hat{\delta}$ and δ_1^β over β_2 , $\hat{\delta}$ and δ_1^β can be parallel to $\tilde{\delta}$ and δ_1^γ respectively. Thus, $t_{\hat{\delta}}^{-(p-2)} t_{\delta_1^\beta}^{p-2} t_{\delta_1^\beta}^{-(p-2)} t_{\delta_1^\gamma}^{p-2}(\beta_1, \beta_2, \beta_3) = (\beta_1, \beta_2, \beta_3)$. In the γ curves, $\tilde{\delta}$ and $\hat{\delta}$ in Figure 17 is obtained by sliding $\tilde{\delta}$ and $\hat{\delta}$ in Figure 16 over γ_2 . This completes the proof. \square

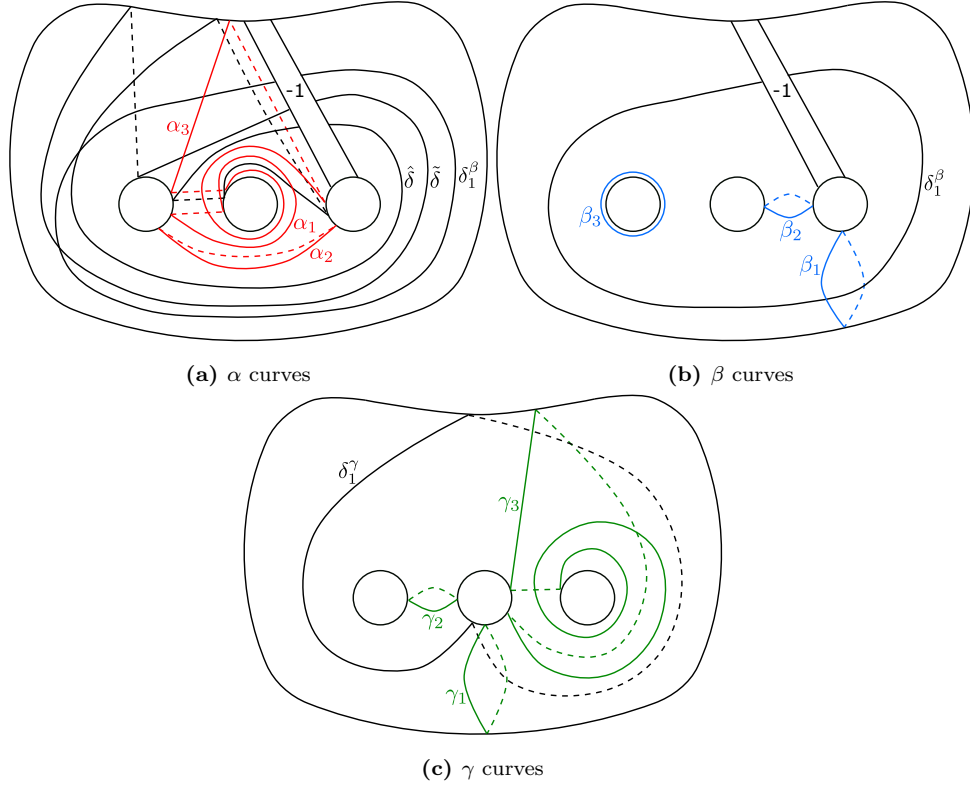


Figure 15. The trisection diagram obtained by the destabilization in the step 2, where $\alpha = (t_{\delta_1^\beta}^{p-2} t_{\tilde{\delta}}^{-(p-2)}(\alpha_1), \alpha_2, t_{\delta_1^\beta}^{p-2} t_{\tilde{\delta}}^{p-2}(\alpha_3))$, $\beta = (t_{\delta_1^\beta}^{p-2}(\beta_1), \beta_2, \beta_3)$ and $\gamma = (t_{\delta_1^\gamma}^{p-2}(\gamma_1), \gamma_2, t_{\delta_1^\gamma}^{p-2}(\gamma_3))$

In Figure 17, $\hat{\delta} = t_m^{-1}(\delta_1^\beta)$ and $\tilde{\delta} = t_m^{-1}(\delta_1^\gamma)$. Thus, $t_{\tilde{\delta}}^{-(p-2)} t_{\hat{\delta}}^{p-2} t_{\delta_1^\beta}^{-(p-2)} t_{\delta_1^\gamma}^{p-2} = t_m^{-1} t_{f_{p-2}(m)}$, where $f_{p-2} = t_{\delta_1^\beta}^{-(p-2)} t_{\delta_1^\gamma}^{p-2} = (t_{\delta_1^\beta}^{-1} t_{\delta_1^\gamma})^{p-2}$. Here, the trisection diagram $((\alpha_1, \alpha_2, \alpha_3), (\beta_1, \beta_2, \beta_3), t_m^{-1} t_{f_{p-2}(m)}(\gamma_1, \gamma_2, \gamma_3))$ is obtained from Lemma 4.6. Then, $((\alpha_1, \alpha_2, \alpha_3), (\beta_1, \beta_2, \beta_3), t_{f_{p-2}(m)}(\gamma_1, \gamma_2, \gamma_3))$ is obtained by performing t_m for the trisection diagram. For this trisection diagram, the following key lemma holds, which we call the seesaw lemma.

Lemma 4.7 (The seesaw lemma). *Let $\alpha = (\alpha_1, \alpha_2, \alpha_3)$, $\beta = (\beta_1, \beta_2, \beta_3)$, $\gamma = (\gamma_1, \gamma_2, \gamma_3)$ in Figure 17. Then, $(\alpha, \beta, t_{f_{p-2}(m)}(\gamma)) = (\alpha, t_m^{-1}(\beta), t_{f_{p-3}(m)}(\gamma))$.*

Proof. We focus on the simple closed curve $f_{p-2}(m)$. By performing $t_{f_{p-2}(m)}^{-1}$ for $(\alpha, \beta, t_{f_{p-2}(m)}(\gamma))$, $(t_{f_{p-2}(m)}^{-1}(\alpha), t_{f_{p-2}(m)}^{-1}(\beta), \gamma)$ is obtained. Then, since $f_{p-2}(m)$ can be parallel to m by sliding $f_{p-2}(m)$ over β_2 $p - 2$ times, $(t_{f_{p-2}(m)}^{-1}(\alpha), t_{f_{p-2}(m)}^{-1}(\beta), \gamma) = (t_{f_{p-2}(m)}^{-1}(\alpha), \beta, \gamma)$. In the α curves, let $\overline{f_{p-2}(m)}$ be simple closed curve obtained by sliding $f_{p-2}(m)$ over α_2 . Namely, $\overline{f_{p-2}(m)} = f_{p-2}(m')$. Then, perform $t_{\overline{f_{p-2}(m)}}$, that is, $(t_{\overline{f_{p-2}(m)}}^{-1}(\alpha), \beta, \gamma) =$

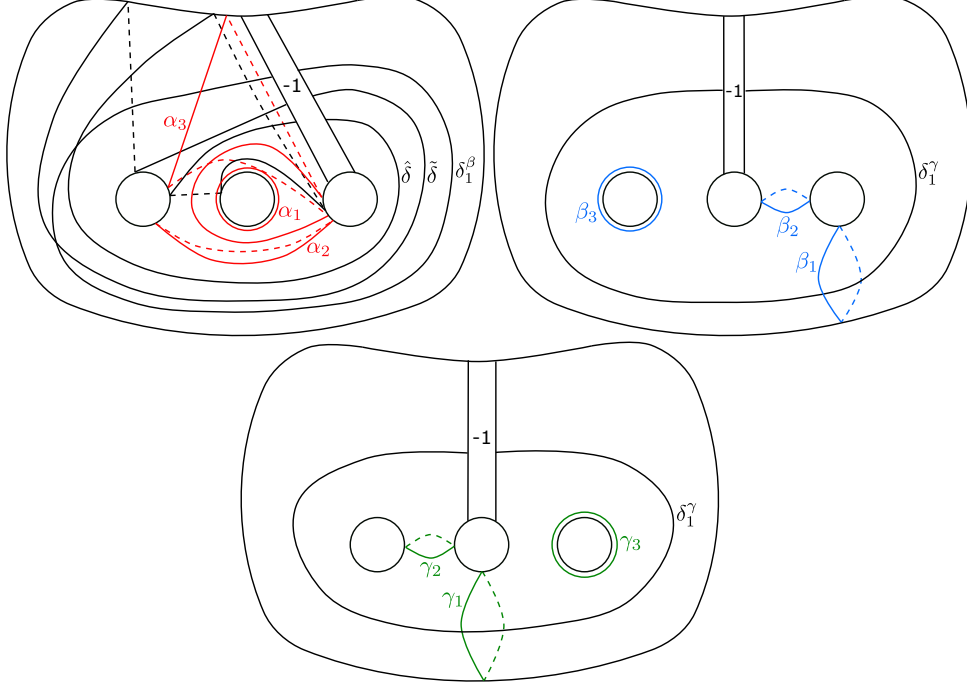


Figure 16. The trisection diagram obtained from Figure 15 after some handle slides and Dehn twists, where $\alpha = (t_{\delta_1^\beta}^{p-2} t_{\delta}^{-(p-2)}(\alpha_1), \alpha_2, t_{\delta_1^\beta}^{p-2} t_{\delta}^{p-2}(\alpha_3))$, $\beta = (t_{\delta_1^\gamma}^{p-2}(\beta_1), \beta_2, \beta_3)$ and $\gamma = (t_{\delta_1^\gamma}^{p-2}(\gamma_1), \gamma_2, t_{\delta_1^\gamma}^{p-2}(\gamma_3))$.

$(t_{f_{p-2}(m)}^{-1}(\alpha), \beta, \gamma) = (\alpha, t_{f_{p-2}(m)}(\beta), t_{f_{p-2}(m)}(\gamma))$. In the β curves, since $f_{p-2}(m)$ can be parallel to m' by sliding $f_{p-2}(m)$ over β_2 $p-2$ times, $(\alpha, t_{f_{p-2}(m)}(\beta), t_{f_{p-2}(m)}(\gamma)) = (\alpha, t_{m'}(\beta), t_{f_{p-2}(m)}(\gamma))$. Moreover, in the γ curves, $f_{p-2}(m)$ can be parallel to $f_{p-3}(m)$ by sliding $f_{p-2}(m)$ over γ_2 since $f_1(m')$ can be parallel to m by sliding $f_1(m')$ over γ_2 . Thus, $(\alpha, t_{m'}(\beta), t_{f_{p-2}(m)}(\gamma)) = (\alpha, t_{m'}(\beta), t_{f_{p-3}(m)}(\gamma))$. This completes the proof. \square

We can use the seesaw lemma iterately since in the proof of the seesaw lemma we only consider handle sliding $f_i(m)$ over α_2 , β_2 and γ_2 . Using the seesaw lemma $p-2$ times for $(\alpha, \beta, t_{f_{p-2}(m)}(\gamma))$, we have $(\alpha, t_{m'}^{p-2}(\beta), t_m(\gamma))$. By performing $t_{m'}^{-(p-2)} t_m^{-1}$ for this trisection diagram, we have (α, β, γ) depicted in Figure 18, the stabilization of the genus 0 trisection diagram of S^4 . This completes the proof of Theorem 4.1.

5. FURTHER REMARKS AND QUESTIONS

In [KM20], Kim and Miller introduced a new technique called a *boundary-stabilization* to construct a relative trisection of the complement of a surface-knot and gave an algorithm for constructing its diagram. Then, they submitted the following question. Note that a P^2 -knot is an embedded real projective plane and the *Price twist* is a cutting and pasting operation along a P^2 -knot. The Price

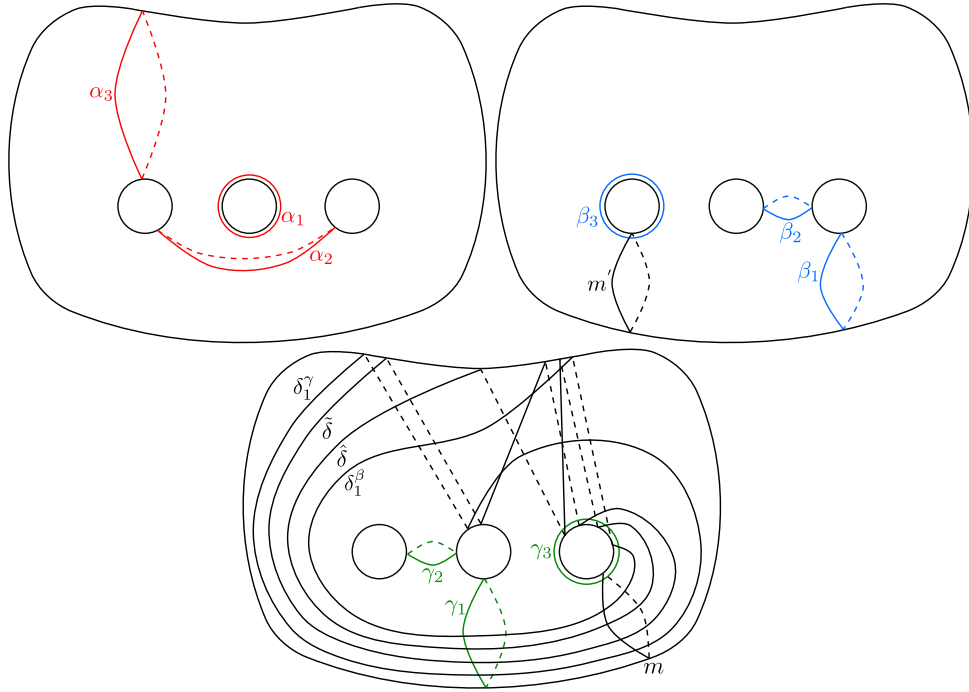


Figure 17. The trisection diagram obtained in Lemma 4.6, where $\alpha = (\alpha_1, \alpha_2, \alpha_3)$, $\beta = (\beta_1, \beta_2, \beta_3)$, $\gamma = t_{f_{p-2}(m)}(\gamma_1, \gamma_2, \gamma_3)$, where $f_{p-2} = t_{\delta_1^\beta}^{-(p-2)} t_{\delta_1^\gamma}^{p-2} = (t_{\delta_1^\beta}^{-1} t_{\delta_1^\gamma})^{p-2}$.

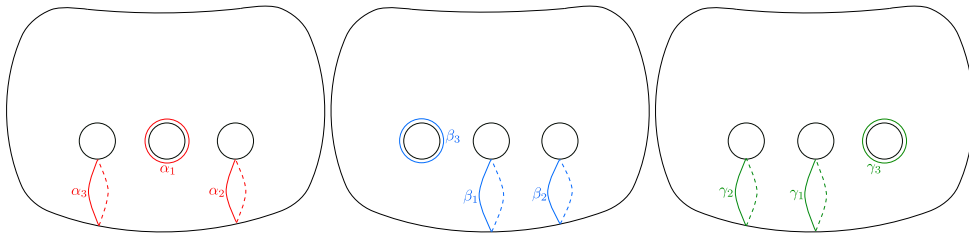


Figure 18. The stabilization of the genus 0 trisection diagram of S^4 .

twist for S^4 on a P^2 -knot S provides us with at most three 4-manifolds up to diffeomorphism, namely, S^4 , a homotopy 4-sphere $\Sigma_S(S^4)$ and $\tau_S(S^4)$ which is not simply-connected.

Question 5.1 (Question 6.2 in [KM20]). Let S be a P^2 -knot in S^4 and $\Sigma_S(S^4)$ the Price twisted homotopy 4-sphere. We consider the case that $\Sigma_S(S^4)$ is diffeomorphic to S^4 . Is a trisection diagram of $\Sigma_S(S^4)$ obtained from the algorithm standard?

It is known that for the unknotted P^2 -knot P and any 2-knot K , $\Sigma_{P\#K}(S^4)$ is diffeomorphic to the Gluck twisted 4-manifold on K [KSTY99]. Naylor [Nay22]

showed that the trisection diagram in Question 5.1 is related to the trisection diagram of the Gluck twisted 4-manifold on K given in [GM22] without stabilizations. Therefore, Theorem 4.1 also answers affirmatively in the case of $S = P\#S(t(p+1, p))$ (and the doubly-pointed trisection diagram). Note that a P^2 -knot $P\#K$ is called of *Kinoshita type*. It is not yet known that any P^2 -knot is of Kinoshita type.

The author and Ogawa [IO23] explicitly depicted the trisection diagram appeared in Question 1.1 in the case of the spun $(2n+1, 2)$ -torus knot, where $n \geq 1$, and showed that the trisection diagram is standard when $n = 1$. (This result corresponds to the case of $p = 2$ in this paper.) However, we have yet to detect whether the trisection diagram is standard when $n \geq 2$. So, we submit the following question:

Question 5.2. Is the trisection diagram of $\Sigma_{S(t(2n+1, 2))}(S^4)$ in [IO23] standard when $n \geq 2$?

Note that in [IO23], we introduced a notion of homologically standard for trisection diagrams and showed that the trisection diagram is homologically standard for all n . Since a standard trisection diagram is homologically standard, the trisection diagram of $\Sigma_{S(t(p+1, p))}(S^4)$ in this paper is obviously homologically standard.

Question 5.3. Is there a non-homologically standard trisection diagram? If No, a homologically standard trisection diagram is standard?

REFERENCES

- [Cas16] Nicolas Andres Castro, *Relative trisections of smooth 4-manifolds with boundary*, Ph.D. thesis, University of Georgia, 2016.
- [CGPC18] Nickolas A. Castro, David T. Gay, and Juanita Pinzón-Caicedo, *Diagrams for relative trisections*, Pacific J. Math. **294** (2018), no. 2, 275–305.
- [GK16] David Gay and Robion Kirby, *Trisecting 4-manifolds*, Geom. Topol. **20** (2016), no. 6, 3097–3132.
- [GM22] David Gay and Jeffrey Meier, *Doubly pointed trisection diagrams and surgery on 2-knots*, Math. Proc. Cambridge Philos. Soc. **172** (2022), no. 1, 163–195. MR 4354420
- [IO23] Tsukasa Isoshima and Masaki Ogawa, *Trisections induced by the Gluck surgery along certain spun knots*, 2023, arXiv:2305.12042.
- [Isl21] Gabriel Islambouli, *Nielsen equivalence and trisections*, Geom. Dedicata **214** (2021), 303–317. MR 4308281
- [Iso22] Tsukasa Isoshima, *Trisections obtained by trivially regluing surface-knots*, 2022, arXiv:2205.04817.
- [KM20] Seungwon Kim and Maggie Miller, *Trisections of surface complements and the Price twist*, Algebr. Geom. Topol. **20** (2020), no. 1, 343–373. MR 4071374
- [KSTY99] Atsuko Katanaga, Osamu Saeki, Masakazu Teragaito, and Yuichi Yamada, *Gluck surgery along a 2-sphere in a 4-manifold is realized by surgery along a projective plane*, Michigan Math. J. **46** (1999), no. 3, 555–571.
- [MSZ16] Jeffrey Meier, Trent Schirmer, and Alexander Zupan, *Classification of trisections and the generalized property R conjecture*, Proc. Amer. Math. Soc. **144** (2016), no. 11, 4983–4997.
- [MZ17] Jeffrey Meier and Alexander Zupan, *Bridge trisections of knotted surfaces in S^4* , Trans. Amer. Math. Soc. **369** (2017), no. 10, 7343–7386.
- [MZ18] ———, *Bridge trisections of knotted surfaces in 4-manifolds*, Proc. Natl. Acad. Sci. USA **115** (2018), no. 43, 10880–10886.
- [Nay22] Patrick Naylor, *Trisection diagrams and twists of 4-manifolds*, C. R. Math. Acad. Sci. Paris **360** (2022), 845–866. MR 4480889
- [Ord13] Philip Ording, *Constructing doubly-pointed Heegaard diagrams compatible with $(1, 1)$ knots*, J. Knot Theory Ramifications **22** (2013), no. 11, 1350071, 26. MR 3143587

DEPARTMENT OF MATHEMATICS, TOKYO INSTITUTE OF TECHNOLOGY, 2-12-1 OOKAYAMA,
MEGURO-KU, TOKYO, 152-8551, JAPAN
Email address: `isoshima.t.aa@m.titech.ac.jp`